


RESEARCH ARTICLE

Intrinsic brain activity patterns across large-scale networks predict reciprocity propensity

Ting Li^{1,2,3} | Zhaodi Pei^{4,5} | Zhiyuan Zhu^{4,5} | Xia Wu^{4,5}  | Chunliang Feng^{1,2} 

¹Key Laboratory of Brain, Cognition and Education Sciences (South China Normal University), Ministry of Education, Guangzhou, China

²School of Psychology, Institute of Brain Research and Rehabilitation (IBRR), Center for Studies of Psychological Application, and Guangdong Key Laboratory of Mental Health and Cognitive Science, South China Normal University, Guangzhou, China

³Institute of Brain and Psychological Sciences, Sichuan Normal University, Chengdu, China

⁴School of Artificial Intelligence, Beijing Normal University, Beijing, China

⁵Engineering Research Center of Intelligent Technology and Educational Application of Ministry of Education, Beijing Normal University, Beijing, China

Correspondence

Chunliang Feng, Key Laboratory of Brain, Cognition and Education Sciences (South China Normal University), Ministry of Education, Guangzhou, China.

Email: chunliang.feng@m.scnu.edu.cn

Xia Wu, School of Artificial Intelligence, Beijing Normal University, Beijing, China.

Email: wuxia@bnu.edu.cn

Funding information

Natural Science Foundation of Guangdong Province, Grant/Award Number: 2021A1515010746; National Natural Science Foundation of China, Grant/Award Numbers: 31900757, 32020103008, 61876021; Fundamental Research Funds for the Central Universities, Grant/Award Number: 2017EYT36

Abstract

Reciprocity is prevalent across human societies, but individuals are heterogeneous regarding their reciprocity propensity. Although a large body of task-based brain imaging measures has shed light on the neural underpinnings of reciprocity at group level, the neural basis underlying the individual differences in reciprocity propensity remains largely unclear. Here, we combined brain imaging and machine learning techniques to individually predict reciprocity propensity from resting-state brain activity measured by fractional amplitude of low-frequency fluctuation. The brain regions contributing to the prediction were then analyzed for functional connectivity and decoding analyses, allowing for a data-driven quantitative inference on psychophysiological functions. Our results indicated that patterns of resting-state brain activity across multiple brain systems were capable of predicting individual reciprocity propensity, with the contributing regions distributed across the salience (e.g., ventrolateral prefrontal cortex), fronto-parietal (e.g., dorsolateral prefrontal cortex), default mode (e.g., ventromedial prefrontal cortex), and sensorimotor (e.g., supplementary motor area) networks. Those contributing brain networks are implicated in emotion and cognitive control, mentalizing, and motor-based processes, respectively. Collectively, these findings provide novel evidence on the neural signatures underlying the individual differences in reciprocity, and lend support the assertion that reciprocity emerges from interactions among regions embodied in multiple large-scale brain networks.

KEYWORDS

individual differences, large-scale networks, machine learning, reciprocity, resting-state fMRI

1 | INTRODUCTION

Reciprocity is often a transmission of prosocial behaviors, referring to a kindness response toward actions perceived to be kind. It reflects a

Ting Li and Zhaodi Pei contributed equally to the current work.

This is an open access article under the terms of the [Creative Commons Attribution-NonCommercial-NoDerivs](https://creativecommons.org/licenses/by-nc-nd/4.0/) License, which permits use and distribution in any medium, provided the original work is properly cited, the use is non-commercial and no modifications or adaptations are made.

© 2022 The Authors. *Human Brain Mapping* published by Wiley Periodicals LLC.

type of social preferences and serves as a fundamental force underlying the evolution of human sociality, such as maintaining cooperation and long-reaching social relations (Bowles & Gintis, 2013; Falk & Fischbacher, 2006; Rand & Nowak, 2013).

In the laboratory setting, reciprocity is measured by well-structured economic exchange games, among which the trust game (TG) is most widely used (Berg et al., 1995). In the TG, a player (the trustor) decides how much to share with another player (the trustee). The shared money is then tripled in value and sent to the trustee. In receipt of the tripled endowment, the trustee decides how much to return back to the investor but, importantly, need not return anything. The amount returned by the trustee is considered as a good indicator to capture individual's reciprocity propensity (Berg et al., 1995; Camerer, 2003). While trustees are obviously better off by betraying, especially in the one-shot TG where there is no opportunity for social reputation building through repeated play, they still adhere to internalized principle of reciprocity at various levels, that is, sending some money back (Cox, 2004; McCabe et al., 2003). Nevertheless, individuals are heterogeneous regarding their reciprocity propensity, and the heterogeneity may depend on a broad of factors, ranging from genetic polymorphisms (Nishina et al., 2019) to testosterone concentrations (Boksem et al., 2013) and personality traits (Ibáñez et al., 2016; Zhao & Smillie, 2015).

Over the past decades, the neuropsychological components underlying the reciprocity behavior have been revealed in combination with TG and neuroimaging techniques (e.g., functional magnetic resonance imaging [fMRI]). In particular, reciprocity decisions are associated with activations of brain regions across multiple large-scale brain networks, including default mode network (DMN; e.g., ventromedial prefrontal cortex [vmPFC]), salience network (SN; e.g., ventrolateral prefrontal cortex [vlPFC]), and fronto-parietal network (FPN; e.g., dorsolateral prefrontal cortex [dlPFC]) (Bellucci et al., 2017, 2019; Declerck et al., 2013; Nihonsugi et al., 2015; van den Bos et al., 2009). For instance, reciprocity may be evoked by inferred good intentions of trustors, engaging mentalizing processes and associated activations in DMN regions (Bellucci et al., 2019; Declerck et al., 2013; Fett et al., 2014). Moreover, reciprocity involves in dealing with the lure of self-interests that strongly drive individuals to betray others. In this regard, betrayal proneness could be addressed either by guilt feelings derived from norm violation (emotion processing, SN) (Bellucci et al., 2017; Phelps et al., 2014; Tangney et al., 2007) or by suppressing selfish motives (cognitive control, FPN) (Nihonsugi et al., 2015; Romano et al., 2017; van den Bos et al., 2009). Taken together, reciprocity may emerge from the interplay of psychological processes associated with mentalizing, emotion processing, and cognitive control.

However, despite the progress in the understanding of neural underpinnings of reciprocity at the group level, personalized investigations of brain function for reciprocity are much less developed. Notably, neural signatures identified at the group do not necessarily reflect individual differences, since group-level studies often treat individual differences as sources of “noise” and discard them by averaging data from a group of participants (Dubois & Adolphs, 2016; Kanai &

Rees, 2011). Therefore, it is important and necessary to investigate individual differences in neural underpinnings of reciprocity with new approaches, especially considering that individuals are widely heterogeneous regarding their reciprocity propensity.

Resting-state fMRI (R-fMRI) is the workhorse to examine neural basis of individual differences. A major reason for the widespread adoption is its minimal requirements (Birn et al., 2013; Dubois & Adolphs, 2016). Moreover, as a task-independent approach, R-fMRI is free from confounds associated with ongoing task demand and different experimental designs across studies (Kable & Levy, 2015; Nash et al., 2014; Nash & Knöchel, 2016), so it is well suitable for quantify individual differences. In contrast, task-dependent approach (e.g., task fMRI) was usually designed to identify group effects that allow inferences about the functions of the “average human brain” (Elliott et al., 2021). Accordingly, a growing number of studies have linked brain activation/connectivity patterns mapped by R-fMRI data to personality traits, cognitive functions and a broad range of social behaviors (Feng et al., 2021b; Hahn et al., 2015; Hsu et al., 2018; Li et al., 2021; Lu et al., 2019; Rosenberg et al., 2016). In the current study, we aimed to examine whether multivariate activation patterns during resting-state predict interindividual variance in the reciprocity propensity.

Resting-state brain activities have been commonly measured by the amplitude of low frequency fluctuations (ALFF; Yu-Feng et al., 2007) and fractional ALFF (fALFF; Zou et al., 2008). These measures reflect the intensity of spontaneous neural activity (Hoptman et al., 2010; Zou et al., 2008) and exhibit higher test–retest reliabilities than other R-fMRI measures, such as the functional connectivity, graph-based network metrics, and voxel-mirrored homotopic connectivity (Chen et al., 2018; Holiga et al., 2018; Somandepalli et al., 2015; Zuo et al., 2010; Zuo & Xing, 2014). Moreover, fALFF/ALFF are well coupling with physiological measures such as cerebral blood flow (Baller et al., 2022; Li et al., 2012; Song et al., 2019) and neuronal glucose metabolism (Aiello et al., 2015; Tomasi et al., 2013). These findings suggest that fALFF/ALFF could capture information on the brain's physiological state and represent potentially meaningful properties of the human brain. Notably, fALFF compared to ALFF overcome the challenge of interfering physiological noise irrelevant to brain activity, and thereby significantly improve sensitivity and specificity in detecting spontaneous brain activities (Zou et al., 2008). Last but not the least, fALFF have been associated with personality traits closely related to reciprocity, including empathy (Cox et al., 2012) and extraversion (Ikeda et al., 2017; Kunisato et al., 2011), which provided a good initial indication of the associations between fALFF and reciprocity. Accordingly, the present work employed fALFF as a proxy for brain activity to predict human reciprocity.

Moreover, given that recent theoretical and empirical evidence indicating that flexible cognitive operations and behavior result from complex interactions within and between large-scale brain networks (Bressler & Menon, 2010; Mišić & Sporns, 2016), we conducted two additional analyses—modularity analysis and functional decoding—after obtaining the regions contributing to predicting reciprocity, which can provide more holistic insights for the contributing regions

from the network level rather than the regional level (Feng et al., 2021a; He & Evans, 2010; Xu et al., 2016). Specifically, modularity analysis with the aid of graph-theoretic approaches was used to investigate whether the regions contributing to predicting reciprocity were segregated into specific brain systems (i.e., modules). Functional decoding analyses to each module was performed based on large-scale data sets in the Neurosynth database (Yarkoni et al., 2011) with the purpose of decomposing distinct neuropsychological components of reciprocity.

In light of previous empirical evidence and theoretical account (Krueger et al., 2008), we hypothesized that patterns of spontaneous activity in multiple brain systems implicated in mentalizing, emotion and cognition function would contribute to predicting individual differences in reciprocity propensity.

2 | MATERIALS AND METHODS

2.1 | Participants

Eighty-six healthy right-handed college students (73 males; 22.62 ± 2.37 years old, range: 18–30 years old) without history of neurological or psychiatric disorder were recruited. The study was conducted in accordance with the 1964 Helsinki Declaration and its later amendments, and was approved by the Ethics Committee of Beijing Normal University. Written informed consents were obtained from all participants. Note that the experimental data were published originally in Feng et al. (2021b), where the analytical strategies and measurements are different from those carried out in the current studies.

2.2 | Trust game

Participants played a one-shot TG (Berg et al., 1995; Camerer & Weigelt, 1988) with a putative anonymous partner. Before the game, participants were given written instructions on the payoff and rules for TG. Afterwards, participants answered several questions designed to assess their understanding of the TG.

Participants acted in the role of trustees and made their decisions in a strategy approach (Brandts & Charness, 2011). Specifically, participants were told that the other player (i.e., trustor) had an endowment of 100 MUs, and needed to decide whether to trust participants or not by passing the endowment to the participants (i.e., trustees). Participants did not know whether the trustor had shared the MUs, but they had to decide how many MUs to return if trustors trusted them. The amount of money returned by trustees measured reciprocity propensity (Berg et al., 1995; Camerer, 2003). It should be noted that in one-shot TG experimental setting, there is no opportunity for punishment or social reputation building. Therefore, a generous returning should be a direct, valid signal of reciprocity or cooperation (Brülhart & Usunier, 2012; Cox, 2004). In particular, a previous study has collected different economic game

decisions from over 1400 individuals, and found that behavioral reciprocity in one-shot TG is highly correlated with self-reported cooperation values, as well as cooperative behavior measured in other experimental paradigms (e.g., Public Goods Game) (Peysakhovich et al., 2014). Moreover, there also existed a strong correlation between the behavioral reciprocity in one-shot TG at different time points (Peysakhovich et al., 2014).

2.3 | Image acquisition

Images were acquired with a Siemens TRIO 3-Tesla scanner at the Beijing Normal University Imaging Center for Brain Research. All participants underwent a 5-min R-fMRI scanning, during which they were instructed to close their eyes, keep still, remain awake, and not to think about anything systematically. The R-fMRI images consisted of 150 contiguous echo-planar imaging volumes using the following parameters: axial slices, 33; slice thickness, 3.5 mm; gap, 0.7 mm; repetition time (TR), 2000 ms; echo time (TE), 30 ms; flip angle, 90° ; voxel size, $3.5 \times 3.5 \times 3.5 \text{ mm}^3$; and field of view (FOV), $244 \times 244 \text{ mm}^2$. In addition, high-resolution structural images were acquired through a three-dimensional sagittal T1-weighted magnetization-prepared rapid acquisition with gradient-echo sequence, using the following parameters: sagittal slices, 144; TR, 2530 ms; TE, 3.39 ms; slice thickness, 1.33 mm; voxel size, $1 \times 1 \times 1.33 \text{ mm}^3$; flip angle, 7° ; inversion time, 1100 ms; and FOV, $256 \times 256 \text{ mm}^2$.

2.4 | Image preprocessing

The R-fMRI data preprocessing was performed using the DPABI software package (Yan et al., 2016), which is a user-friendly toolbox based on SPM (SPM12, <https://www.fil.ion.ucl.ac.uk/spm/>). Firstly, considering signal equilibrium and participants' adaptation to scanning noise, the first 10 time points of the images were removed. The realignment was then performed for head motion correction. Four participants were excluded according to the criteria of head motion exceeding 2.5 mm maximum translation, 2.5° rotation or mean frame-wise displacement (FD) exceeding 0.2 mm over the process of scans (Power et al., 2012; Yan et al., 2013). For spatial normalization, the structural images of participants were co-registered to corresponding functional images and were subsequently segmented. The parameters obtained from segmentation were afterwards applied to normalize participants' functional images into the Montreal Neurological Institute (MNI) space (MNI template with a resolution of $3 \times 3 \times 3 \text{ mm}^3$). After that, the constant and linear trends of time courses were removed. Moreover, the Gaussian smooth filter was used to reduce the influence of spatial noise (full-width at half maximum [FWHM] = $4 \times 4 \times 4$). Finally, three nuisance variables were regressed out, including white matter signal, cerebrospinal fluid signal and 24 movement regressors consisting of six head motion parameters, six head motion parameters one time point before and the 12 corresponding squared items (Friston et al., 1996).

2.5 | Calculation of fALFF

In ALFF analysis, the time series of each voxel were firstly converted to the frequency domain and the power spectrum was obtained. Then the square root of the power spectrum was computed and the mean value of square root ranging from 0.01 to 0.08 Hz for each voxel was obtained as ALFF (Yu-Feng et al., 2007). It was indicated that the amplitude of low-frequency fluctuation of the R-fMRI signals could reflect the intensity of regional spontaneous brain activity (Hoptman et al., 2010). However, the ALFF is also sensitive to the physiological noise. Therefore, an improved method named fALFF was proposed (Zou et al., 2008). In particular, fALFF was defined as the ratio of the power of the low-frequency range (0.01–0.08 Hz) to that of the entire frequency range (0–0.25 Hz). Compared with the ALFF, it was demonstrated that the fALFF could repress nonspecific signals in the R-fMRI, and therefore would significantly improve the sensitivity and specificity in detecting regional spontaneous brain activity (Zou et al., 2008). The procedure of data analysis of fALFF was similar to that of ALFF, with the additional step that the sum of amplitude at low-frequency across 0.01–0.08 Hz was divided by that across the entire frequency range (0–0.25 Hz) (Yan, 2010).

In this study, regions of interest (ROIs) were defined by using a functional atlas of human brain (Power et al., 2011). This atlas, which is yielded with the hypothesis that a graph represents some features of brain organization, includes 264 ROIs spanning the cerebral cortex, subcortical structures, and the cerebellum. ROIs were generated as 10 mm diameter spheres and each of them was on behalf of an element of brain organization (Power et al., 2011). For each ROI, fALFF was calculated by averaging the value of all the voxels that the ROI comprises.

2.6 | Predictive model

In the present study, ridge regression linear model was applied to predict participants' reciprocity propensity measured with the TG from regional spontaneous brain activity (i.e., fALFF). The ridge regression has been widely used for predictions in the neuroimaging field (Cui & Gong, 2018; Siegel et al., 2016; Yang et al., 2016). Specifically, linear regression model could be used to predict the individual reciprocity propensity using the fALFF features extracted from ROIs across the whole brain. The linear model can be formulated as follows:

$$\hat{Y} = \sum_{i=1}^P \beta_i X_i + \beta_0,$$

where \hat{Y} is the prediction of individual reciprocity propensity, X_i is the fALFF value at the i th ROI, P is the number of ROIs obtained across the whole brain, and β_i is the regression coefficient.

For higher prediction accuracy and avoidance of overfitting, regularization techniques have been widely applied in model fitting (Hoerl & Kennard, 1970). The formula is as follows:

$$\min_{\beta} \sum_{i=1}^N (\hat{y}_i - y_i)^2 + \lambda \sum_{j=1}^P \|\beta_j\|^2,$$

where y_i is the real reciprocity propensity of the i th individual, and N is the number of training samples. The regularization parameter λ is able to adjust the compromise between the prediction error and the L2 regularization. In the ridge regression, the purpose of the L2 regularization is to minimize the sum of the square of the regression coefficients and therefore to improve the generalizability for predicting unseen data. Compared with traditional models such ordinary least squares, the ridge regression can better cope with the problem of multicollinearity and overfitting (Vinod, 1978). Consequently, the ridge regression model was commonly used in the prediction based on neuroimaging measures for its stable performance and avoidance of overfitting (Cui & Gong, 2018).

2.7 | Prediction framework

The schematic diagram of the prediction framework is shown in Figure 1. Concretely, for each subject, the fALFF values of all ROIs were drew to form a feature vector. Subsequently, feature vectors of all subjects were combined to get a feature matrix. Then the 10-fold cross validation was used to test the ability of model to predict unseen individuals, since it may provide more stable estimates of predictive accuracy (Varoquaux et al., 2017). Specifically, all subjects were divided into 10 subsets, in which 9 subsets were served as the training set and the left one was used as the testing set. This procedure was repeated 10 times in order to make sure that each subset was used as the testing set once.

In order to measure the accuracy of prediction, Pearson correlation coefficient (r) and mean absolute error (MAE) between predicted and actual reciprocity propensity were calculated. Considering the full data set were divided randomly, the performance might depend on the data division. Consequently, the process of 10-fold cross validation was repeated 100 times, and the results were averaged to obtain a final prediction performance. Furthermore, permutation test was used to determine whether the obtained accuracy metrics were significantly better than expected by chance. Specially, the procedure of prediction was repeated 5000 times and in each time the behavior scores across all participants were permuted without replacement. The p value was finally computed by dividing the number of permutations that performed greater (or in the case of MAE, less) than the true value by the total number of permutations (i.e., 5000).

Moreover, the leave-one-out cross validation (LOO-CV) was performed to supplement our main findings. Specifically, there were $N - 1$ subjects served as the training set and the remaining one subject served as the testing set, where N is the number of subjects. This procedure was repeated N times so that each subject can be used once as testing set and as much valid information as possible can be obtained from limited data (Finn et al., 2015; Siegel et al., 2016). Similarly, the Pearson correlation coefficient (r) and MAE was computed

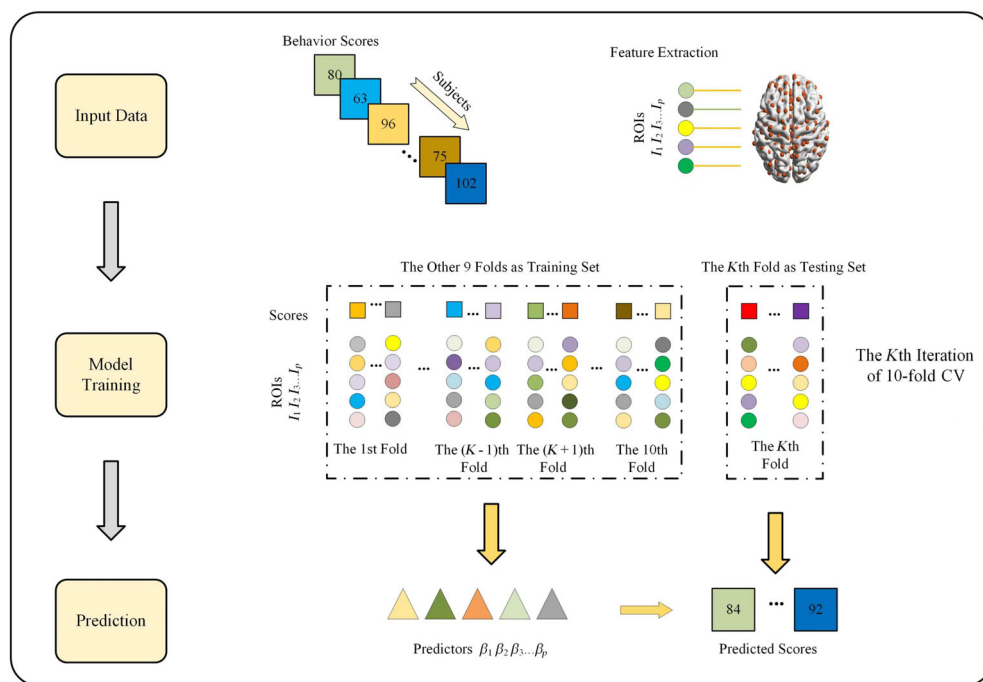


FIGURE 1 Prediction scheme. Step 1 (feature extraction): The mean fractional amplitude of low frequency fluctuations (fALFF) of 264 regions of interest (ROIs) in the Power atlas (Power et al., 2011) was extracted as prediction features of each participant. Step 2 (model construction): The relationship between fALFF and reciprocity propensity was examined using ridge regression linear model, combining with the 10-fold cross-validation to assess the prediction performance. Step 3 (model evaluation): The accuracy of prediction was measured by the correlation coefficient (r) and mean absolute error (MAE).

between the true and predicted values, and a 5000 times permutation test was applied to examine the significance of the prediction performance.

2.8 | Contributing regions in the prediction

The prediction weights of ROIs derived from the model represent parameters of the backward models, in which latent factors were extracted from the observed data. It has been demonstrated that the original weights of backward models (e.g., ridge regression model in the current study) do not necessarily indicate the contribution of the corresponding features (Haufe et al., 2014). Accordingly, Haufe et al. (2014) proposed an algorithm to reconstruct activation patterns from the original weights, so that the resultant activation patterns could be interpreted to indicate the significance of each feature to the prediction model.

Moreover, the stability of the features was evaluated using a bootstrap test (Kohoutová et al., 2020) based on the scores of activation patterns. In particular, a total of 10,000 bootstrap samples was generated by sampling randomly with replacement and trained a model for each sample to get a distribution of the activation patterns for each brain region. Then the quotient (i.e., z and p) of the mean and the standard deviation of bootstrap distributions for each region were calculated as a measure of the feature stability. Based on the bootstrap results, a threshold of $p < .05$ (i.e., $|z| > 1.96$) was determined to select features for display purpose (see also Karlaftis et al., 2019). This threshold was selected due to the reason that a sparse pattern derived from the pattern was sufficient to predict reciprocity propensity with comparable sensitivity to the full model (see also Chang et al., 2015). It should be noted that, as in previous

neuroimaging-based prediction studies, the features were only selected for display purpose (e.g., Chang et al., 2015; Chen et al., 2021; Karlaftis et al., 2019; Wager et al., 2013; Woo et al., 2014; Woo et al., 2017).

The revealed features (i.e., brain regions) were further validated by establishing two new prediction models. In the first model, only the 24 revealed brain regions (see also Results) were employed in the prediction model. In the second model, the revealed regions were excluded, and the remaining regions were employed in the prediction model. The predictive performance of these models (also known as “virtual lesion analysis”) was compared with full model to indicate the significance of the revealed brain regions (see also Kohoutová et al., 2020).

2.9 | Module detection

Furthermore, to investigate whether these contributing ROIs are uniformly interconnected or ulteriorly segregated into modules in which the connections between ROIs are much denser, we performed a modularity analysis with spectral optimization algorithm using the Graph-theoretical Network Analysis Toolkit (He et al., 2009; Wang et al., 2015). Concretely, for each participant, the resting-state functional connectivity (RSFC) matrix between 24 regions listed was firstly computed. For following analysis, matrixes across all participants were Fisher z -transformed and averaged to generate a mean functional connectivity matrix of 24×24 . Moreover, the diagonal and negative links of the mean RSFC matrix were set to zero (Power et al., 2011, 2013; Rubinov & Sporns, 2010). To exclude the confounding impact of spurious relationships in international connectivity matrixes, a threshold procedure was applied. Specifically, we set the initial value

of connectivity density to the lower qualification when the graph begins to split into components and increased it by 0.01 to 0.5 so as to examine the network stability (Xu et al., 2016). Here, starting with the value of 0.31, contributing regions are completely confined to one of modules.

2.10 | Functional decoding for identified modules

To explore which psychological topics were most relevant to each identified module of modular analysis, a functional decoding analysis was performed based on the Neurosynth database (version 0.6) (Yarkoni et al., 2011) with codes from a set of IPython Notebooks (<https://github.com/adelavega/neurosynth-lfc>) (de la Vega et al., 2018). Neurosynth is a framework for large-scale fMRI meta-analysis, consisting of 11,406 studies that cover all-sided published neuroimaging literature (Yarkoni et al., 2011). For each fMRI study, peak coordinates of all activations and the frequency of all words in the article abstract were collected in the Neurosynth database. Based on the co-occurrence of all words in the abstracts, 60 independent psychological topics were ultimately obtained to remedy the redundancy and potential ambiguity using latent Dirichlet allocation topic modeling (de la Vega et al., 2018). First, we generated three brain masks consisting of regions in the module central execution network (CEN), module DMN, and module somatic sensorimotor network (SSM) (see Results), respectively. For each brain mask, two sets of studies were then selected that either activated at least 5% of voxels (active studies) or did not activate any voxel (inactive studies) within the mask. Subsequently, a naive Bayes classifier was trained to discriminate the two sets of studies on the basis of the loading of each psychological topic onto individual studies. This resulted in 60 log odds-ratio (LOR) values for each brain mask calculated as the log of the ratio between the probability of each topic in active studies and the probability of that topic in inactive studies. A LOR value greater than zero indicated that the corresponding psychological topic was predictive of whether a study activated regions in a given brain mask when the semantic content of the study was known. Finally, a permutation-based method was used to determine significance level for the observed LOR values by reshuffling study labels (i.e., active or inactive) (1000 times). Noting that, only those top six topics that yielded significant result ($p < .01$) in multiple comparisons using false discovery rate were reported.

2.11 | Control analysis

Control analysis was implemented to further examine the significance of predictions of our models, despite potential confounds of head motion (mean FD), age, and gender. In the control analysis, the association between actual and predicted reciprocity propensity was re-computed after adjusting these confounding variables.

3 | RESULTS

3.1 | Prediction analysis with cross validation

The method of 10-fold cross-validation was applied to examine whether the correlation between fALFF and participants' reciprocity propensity could generalize to novel individuals. The result shows that fALFF features were able to predict new individuals' reciprocity propensity ($r = 0.26$, $p = .0044$; $MAE = 22.80$, $p = .0018$, permutation test). The prediction remained after adjusting for head motion, age, and gender ($r = 0.26$, $p = .0046$; Figure 2a,b; $MAE = 22.53$, $p = .0012$; Figure 2c,d, permutation test). Similar results were identified with the LOO-CV (unadjusted for covariates: $r = 0.28$, $p = .0016$; $MAE = 22.40$, $p = .0004$, permutation test; adjusted for covariates: $r = 0.28$, $p = .0014$; $MAE = 22.04$, $p = .0004$, permutation test).

3.2 | Contributing regions in the prediction

Both the original weights (all $r > 0.85$) of the prediction model and reconstructed activation patterns (all $r > 0.89$) were highly correlated among folds, suggesting that the contributing regions of the prediction model were stable across cross-validation folds.

As illustrated in Table 1, the bootstrap test identified 24 ROIs that stably contribute to the prediction model. Notably, a new model was trained by employing the revealed regions only, which resulted in a much better predictive performance with the full model ($r = 0.61$, $p < .0002$, permutation test). In contrast, another model excluding the identified regions performed worse than the full model ($r = -0.29$, $p = .98$, permutation test). Therefore, the complementary findings supported the significance of the identified brain regions.

3.3 | Network analysis for contributing regions

To further examine the network structures of contributing regions in prediction, modularity analysis was performed on the RSFC matrix across series of thresholds. As shown in Figure 3a, the module structure under connectivity density levels from 0.31 to 0.50 with a step of 0.01 was plotted and three distinct, as well as stable, modules were obtained across all thresholds tested. Figure 3b–d illustrated the results under the connectivity of 0.40, when all the ROIs were divided into the most common modules ($N = 3$). In Figure 3c, ROIs located in the plane according to connectivity patterns. The three modules obtained were distinguished from each other clearly. Figure 3d represented the functional connectivity matrix. It was shown that three densely connecting modules could be captured against with the background, demonstrating the stronger connections within modules in comparison to connections between modules.

Figure 3b showed spatial location of three modules on the brain surface in which the colors of ROIs represented different modules. First, the module 1 colored blue mainly consisted of vIPFC, anterior prefrontal cortex (antPFC), orbitofrontal cortex (OFC), dIPFC,

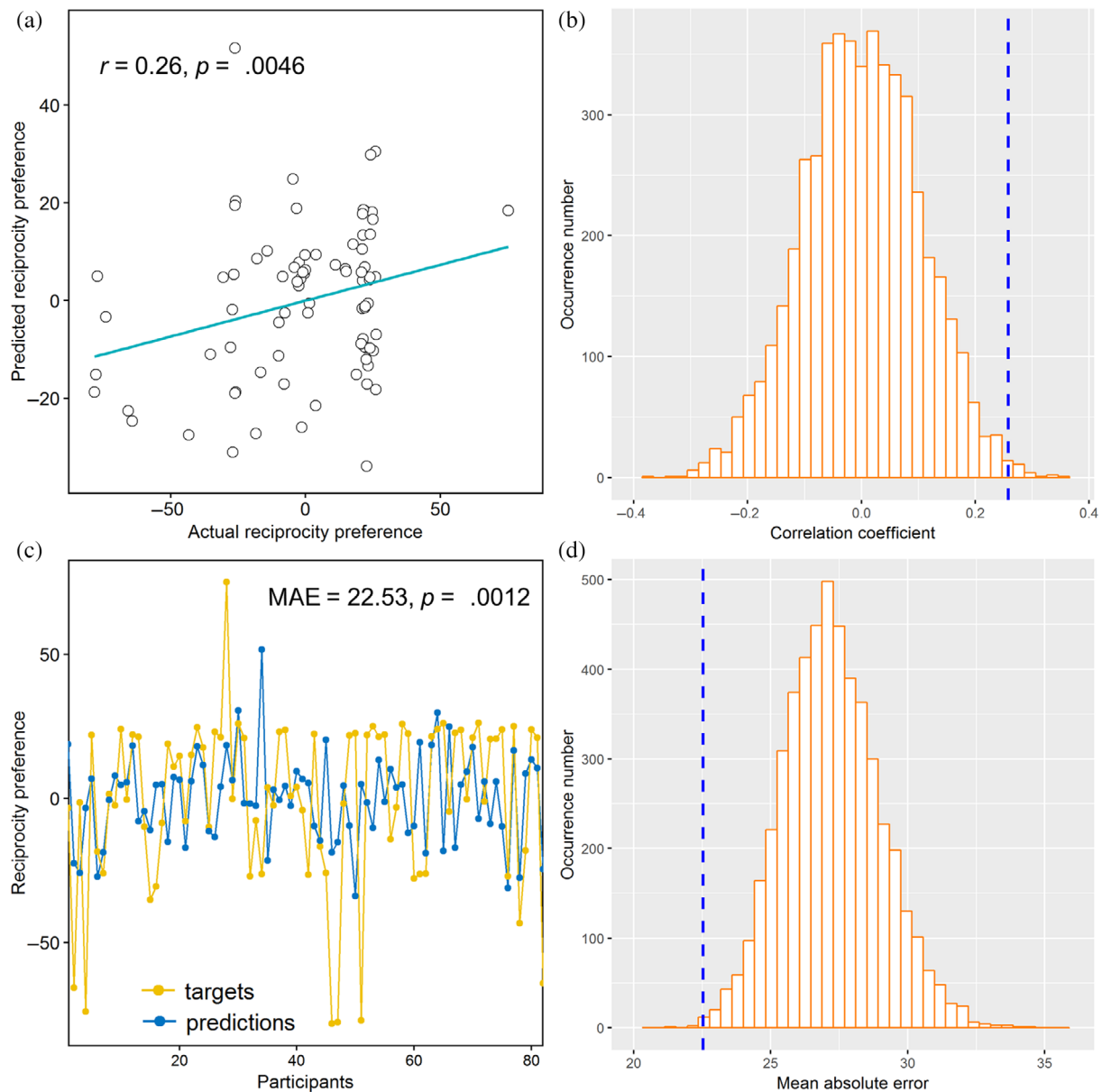


FIGURE 2 Results of 10-folds cross validation (CV). (a) The relationship between predicted reciprocity scores and actual reciprocity scores based on fractional amplitude of low frequency fluctuation (fALFF) features. (b) Permutation distribution of the prediction accuracy with the blue dashed line indicating the value obtained from real reciprocity scores. (c) Consistency between prediction scores and actual reciprocity scores. (d) Permutation distribution of the mean absolute error (MAE) with blue dashed line indicating the value obtained from real reciprocity scores.

posterior parietal cortex (PPC), inferior temporal gyrus (ITG), and putamen. These regions mostly located in the areas of SN and FPN in the atlas, which could be merged here as the CEN for tabular and graphical visualizations. Second, the module 2 colored yellow mainly included vmPFC, posterior cingulate cortex (PCC), and cerebellum, which mostly located in the areas of DMN. The module 3 coded red basically comprised supplementary motor area (SMA), middle occipital gyrus (MOG), precentral gyrus, postcentral gyrus, cuneus, and fusiform, which mostly spread in SSM.

Figure 4 illustrated the functional profiling of regions contributing to predicting reciprocity propensity. Module CEN was mostly associated with decision-making, working memory, switching, inhibition,

arithmetic, and fear. Module DMN was mostly related to awareness, memory, semantic, reading, disorders, and motor. Module SSM was mostly linked to motor, visual-motor, body, spatial, action, and face/emotion.

4 | DISCUSSION

Reciprocity encourages social interaction in a cooperative fashion among individuals across human societies; however, people usually exhibit widely heterogeneous reciprocity propensity. At the neural level, the neurobiological markers of this heterogeneity remain largely

TABLE 1 Contributing ROIs in the prediction. ROIs are sorted by modules, and the activation patterns were thresholded using a 10,000-sample bootstrap procedure at $p < .05$ uncorrected

Module	ROI label	Hemisphere	MNI space			Activation pattern
			X	Y	Z	
CEN	VLPFC/OFC	R	43	49	-2	-0.20
CEN	antPFC	L	-39	51	17	-0.16
CEN	VLPFC/IFGorb	R	36	22	3	-0.14
CEN	DLPFC/MFG	L	-42	38	21	-0.13
CEN	PPC/IPL	R	44	-53	47	-0.14
CEN	PPC/IPL	R	49	-42	45	-0.11
CEN	VLPFC/IFGorb	R	34	16	-8	-0.07
CEN	VMPFC/OFC	L	-21	41	-20	-0.09
CEN	ITG	R	58	-53	-14	-0.15
CEN	Putamen	R	31	-14	2	-0.10
DMN	PCC	L	-3	-49	13	0.18
DMN	PCC	R	8	-48	31	-0.17
DMN	VMPFC/IFGorb	R	-46	31	-13	0.10
DMN	Cerebellum	L	-18	-76	-24	-0.12
DMN	Cerebellum	R	17	-80	-34	-0.08
DMN	Cerebellum	R	35	-67	-34	-0.14
DMN	Cerebellum	R	22	-58	-23	-0.11
SSM	SMA	L	-13	-17	75	-0.12
SSM	MOG	R	29	-77	25	-0.11
SSM	Precentral/M1	R	29	-17	71	0.12
SSM	Precentral/M1	L	-23	-30	72	-0.14
SSM	Postcentral/S1	R	50	-20	42	0.09
SSM	Cuneus	L	-16	-77	34	-0.13
SSM	Fusiform	R	46	-47	-17	-0.12

Abbreviations: antPFC, anterior prefrontal cortex; CEN, central execution network; dIPFC, dorsolateral prefrontal cortex; DMN, default-mode network; IFGorb, inferior frontal pars orbitalis; IPL, inferior parietal lobe; ITG, inferior temporal gyrus; MFG, medial prefrontal cortex; MNI, Montreal Neurological Institute; MOG, middle occipital gyrus; OFC, orbitofrontal cortex; PCC, posterior cingulate cortex; PPC, posterior parietal cortex; SMA, supplementary motor area; SSM, sensorimotor network; vIPFC, ventrolateral prefrontal cortex; vmPFC, ventromedial prefrontal cortex.

unknown. Here, combining the neuroimaging and machine learning techniques, we investigated whether individual differences in reciprocity propensity could be predicted by resting-state brain activity (i.e., fALFF) across brain regions. We found that individual reciprocity propensity could be predicted by multivariate patterns of resting-state brain activity of multiple regions across distributed brain systems, including vIPFC, antPFC, OFC, dIPFC, PPC, ITG, putamen, vmPFC, PCC, SMA, MOG, precentral gyrus, postcentral gyrus, cuneus, fusiform, and cerebellum. Modular analysis revealed that these regions were organized into three stable modules, corresponding to the CEN (it should be noted that the CEN is divided into SN and FPN), DMN, and SSM, which were respectively implicated in emotion processing and cognitive control, mentalizing, and motor-based processes. Together, in addition to demonstrating that resting-state features provide reliable neuromarkers of human reciprocity propensity, these findings advance our understanding of reciprocity and prosocial behaviors in terms of large-scale brain networks.

First, the module CEN comprised of vIPFC, antPFC, OFC, dIPFC, PPC, ITG, and putamen mainly located in SN and FPN, which was associated with emotion processing and cognition control revealed by our functional decoding analyses. In the social dilemma between maximizing and sacrificing personal benefits, impulses of betrayal (e.g., violating reciprocity norm) are pervasive. However, this dilemma could be resolved with the emotional processing and cognitive control implemented in the SN and FPN respectively. On one hand, emotion plays a critical role in the establishment of response-dependent values and norm compliance (FeldmanHall et al., 2018; Heffner et al., 2021; Phelps et al., 2014). Accordingly, the experience or anticipation of moral emotion derived from norm violation, such as guilt feelings, may be a potent motivator for upholding reciprocity (Chang et al., 2011; FeldmanHall et al., 2018; Krueger et al., 2020). For instance, greater guilt sensitivity was associated with increased recruitment of SN regions (e.g., vIPFC; Wagner et al., 2011), while diminished guilt aversion corresponded to lessened reciprocal behavior (Gong et al., 2019).

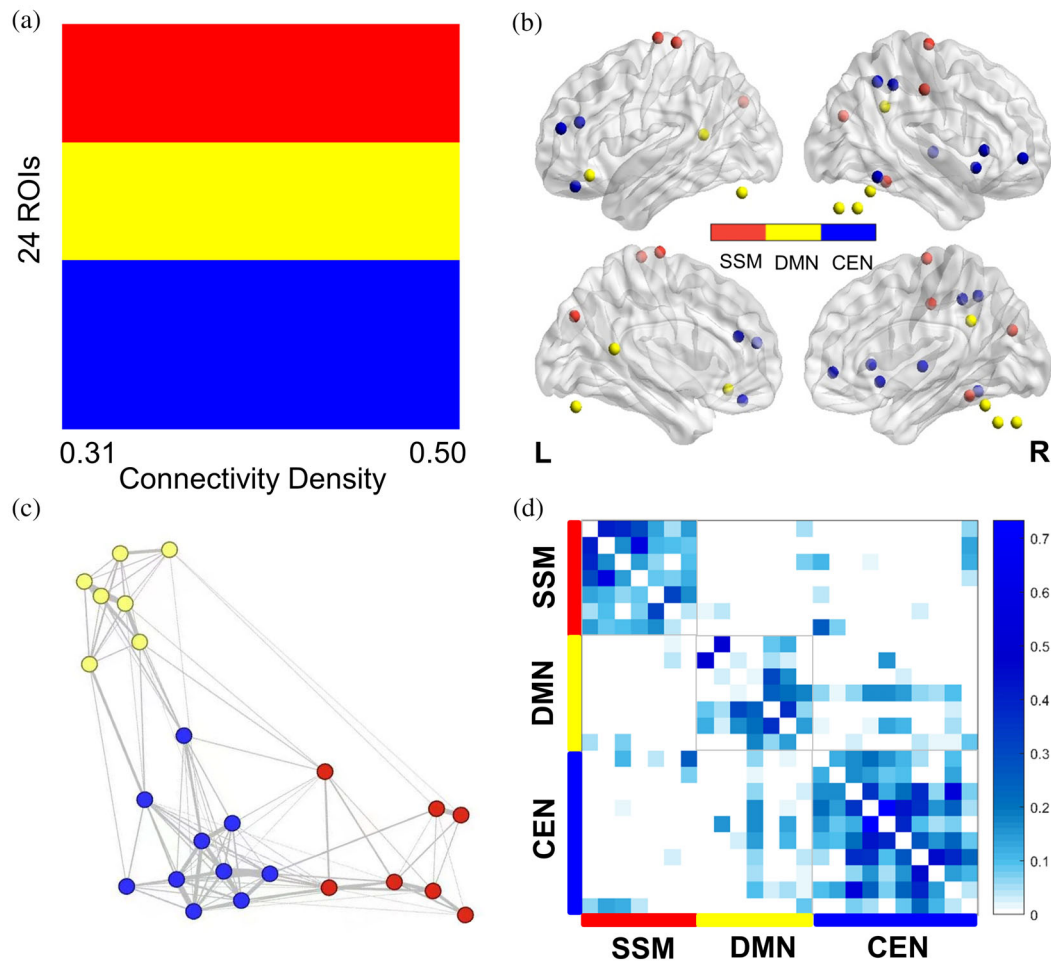


FIGURE 3 Results of modularity analysis. (a) The modularity analysis determined three stable modules from regions of interest (ROIs) shown in the same color (CEN, blue; DMN, yellow; SSM, red) under connectivity density levels ranging from 0.31 to 0.50 by increments of 0.01. (b) The fALFF-based prediction model determined 24 contributing regions (i.e., ROIs). The colors indicate different brain network modules. (c) The spring-like layout of the three network modules for a connectivity density of 0.40 displays the Euclidean distance between each pair of nodes. The thickness of lines indicates the connection strength of the edges. (d) Functional connectivity matrix for a connectivity density of 0.40 (ROIs are sorted by modules) showing a stronger strength of edges within than those between modules. CEN, central execution network; DMN, default-mode network. L, left; R, right; ROIs, regions of interest; SSM, sensorimotor network.

On the other hand, given the importance of cognitive control for cooperation maintenance, reciprocity could be facilitated by suppressing selfish motives (Fett et al., 2014; van den Bos et al., 2011). In accordance, evidence from previous task fMRI studies has indicated that important FPN regions (e.g., dIPFC) were recruited in reciprocity (van den Bos et al., 2009). Moreover, enhancement of dIPFC excitability resulted in increased reciprocity (Nihonsugi et al., 2015), whereas transient disruptions of the dIPFC led individuals to send less money back, even if they know it is harmful to their future social reputation (Knoch et al., 2009). To sum up, our results suggest that SN and FPN (or collectively called module CEN) play important roles in reciprocity through emotional processing and cognitive control, facilitating individuals to make reciprocal decisions in favor of long-term social relationships.

Second, the module DMN consisted of PCC, vmPFC, and cerebellum, which overlapped with canonical DMN and was mainly

associated with mentalizing revealed by our functional decoding analyses. Mentalizing is essential for reciprocity by modeling others' mental states (Beer & Ochsner, 2006). Accordingly, reciprocity decisions were associated with enhanced activity in the regions of DMN (e.g., PCC, vmPFC) in both TG and the prisoner's dilemma game (King-Casas et al., 2005; Krueger et al., 2007; Rilling et al., 2004; Rilling et al., 2008). In addition, functional connectivity of DMN was associated with individual differences in reciprocal behavior (Schreiner et al., 2014) and understanding the concept of reciprocity (Bisecco et al., 2019). Consequently, it is conceivable that mentalizing processes mediated by the DMN allows individuals to predict the experiences, beliefs, and intentions of the other, and to promote reciprocal behaviors in the context of social interaction.

Finally, the module SSM consisted of SMA, MOG, precentral gyrus, postcentral gyrus, cuneus, and fusiform, which was primarily embedded in the SSM and associated with motor-based processes.

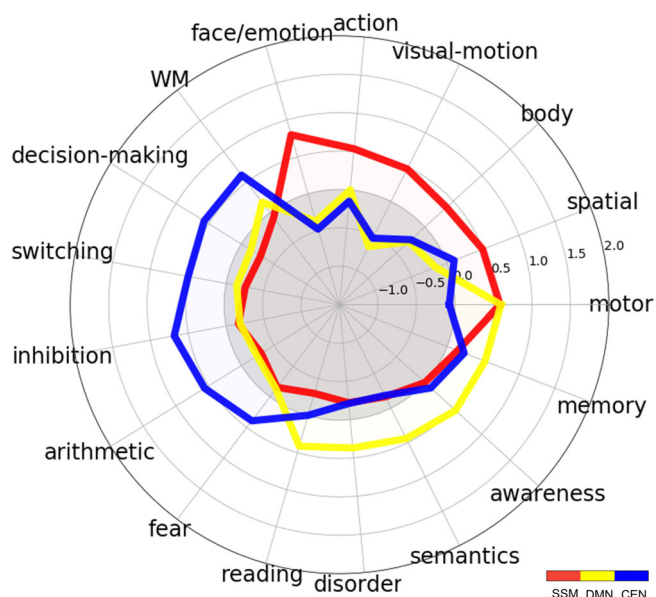


FIGURE 4 Results of functional decoding. The log odds ratio between the probability of a given topic activating the network was displayed in a functional decoding profile for each network. CEN, central execution network; DMN, default-mode network; SSM, sensorimotor network. WM, working memory.

Although few previous studies have directly reported a relationship between human reciprocity and SSM, the engagement of SSM is actually not surprising (Iacoboni & Dapretto, 2006; Pineda, 2008), since reciprocity occurs in human social interactions that require the execution of action and perception of actions of others. Evidence from neuroimaging study has demonstrated that active engagement in a social interaction, compared with observation of social stimuli, activates a more extensive network of areas associated with motor perception and action, which in turn promotes motor responses coherent with the social stimuli (Schilbach et al., 2013). In addition, early intervention targeting the ability of sensorimotor processes could positively support social development (Cerullo et al., 2021); rather, individuals exhibiting poor motor performances have difficulty in acquiring essential social skills (e.g., reciprocity and communication), and this effect could be mediated by the function, structural integrity, and connectivity of motor brain regions and networks (Biotteau et al., 2019; Kilroy et al., 2019). For example, autism spectrum disorders showed altered connectivity between SSM and cerebellum compared to healthy controls; moreover, disrupted functional connectivity within the SSM could account for autism symptoms, including atypical sensory processing, repetitive behaviors, and social impairments (Oldehinkel et al., 2019). These findings are consistent with the hypothesis of action-perception matching or action simulation, holding that the SSM contributes to the understanding of others' intentions or emotions by partially reproducing experienced actions or emotional expressions in one's own (Davis et al., 2017; Oliver et al., 2018). In short, the motor-based processes play a critical role in promoting socially adaptive responses during social interactions, and the current findings

complement this idea by highlighting the associations between SSM and reciprocity.

Several limitations related to the current study should be noted. First, we found that the resting-state brain activity (i.e., fALFF) could predict individual variations of reciprocity propensity measured by one-shot TG in a single group. Future studies are required to validate the reproducibility of our prediction model on a new, independent sample, and to explore whether the fALFF-reciprocity associations are stable, and independent of the experimental setting of one-shot TG and multi-round TG. Second, although our prediction model worked well in predicting reciprocity propensity, we noted that the deviations between the predicted values and real observations were relatively large for some data points. One possible reason is that the current prediction model only employed the fALFF as prediction features. A more robust and accurate prediction model in future studies might be constructed by combining more modalities of features (e.g., functional connectivity, regional homogeneity [ReHo], and ALFF) or considering connectivity and graph-based network measures. Moreover, it is also interesting for future studies to systematically compare the predictive performance of different modalities of features in reciprocity propensity. Third, only a small group of females was included in the current study, and future studies are needed to recruit comparable male and female participants to avoid the risk of gender-biased results. Finally, this study focused on the relationships between resting-state brain activity and individual reciprocity propensity in healthy participants. Nevertheless, social skills deficits are hallmark symptoms of mental disorders. It is interesting for future studies to explore whether the fALFF could be used to identify the neural marker of mental disorders characterized by social dysfunction (e.g., autism).

Despite of these limitations, our study provided the evidence that fALFF features of multiple brain regions enabled prediction of reciprocity propensity at individual level. Our study further identified brain systems underlying the individual differences in reciprocity, including SN, FPN, DMN, and SSM. The modules are implicated in emotion processing and cognitive control, mentalizing, and motor-based processes. These findings shed light on the neurocognitive mechanisms underlying human reciprocity, and advance our understanding of reciprocity from the perspective of network integration.

AUTHOR CONTRIBUTIONS

All authors contributed to the study conception and design. Material preparation, data collection, and analysis were performed by Chunliang Feng and Zhaodi Pei. The first draft of the manuscript was written by Ting Li and Zhaodi Pei, and all authors commented on previous versions of the manuscript. All authors read and approved the final manuscript.

ACKNOWLEDGMENTS

Chunliang Feng was supported by the Natural Science Foundation of Guangdong Province (2021A1515010746) and the National Natural Science Foundation of China (31900757, 32020103008). Xia Wu was supported by the National Natural Science Foundation of China

(61876021) and Fundamental Research Funds for the Central Universities (2017EYT36).

CONFLICT OF INTEREST

The authors declare that they have no conflict of interest.

DATA AVAILABILITY STATEMENT

The data that support the findings of this study are available from the corresponding author upon reasonable request. Because of restrictions based on privacy regulations and informed consent of the participants, the data cannot be made freely available in a public repository.

ORCID

Xia Wu  <https://orcid.org/0000-0002-2377-6093>

Chunliang Feng  <https://orcid.org/0000-0001-5595-2146>

REFERENCES

- Aiello, M., Salvatore, E., Cachia, A., Pappatà, S., Cavaliere, C., Prinster, A., Nicolai, E., Salvatore, M., Baron, J.-C., & Quarantelli, M. (2015). Relationship between simultaneously acquired resting-state regional cerebral glucose metabolism and functional MRI: A PET/MR hybrid scanner study. *NeuroImage*, 113, 111–121. <https://doi.org/10.1016/j.neuroimage.2015.03.017>
- Baller, E. B., Valcarcel, A. M., Adebimpe, A., Alexander-Bloch, A., Cui, Z., Gur, R. C., Gur, R. E., Larsen, B. L., Linn, K. A., O'Donnell, C. M., Pines, A. R., Raznahan, A., Roalf, D. R., Sydnor, V. J., Tapera, T. M., Tisdall, M. D., Vandekar, S., Xia, C. H., Detre, J. A., ... Satterthwaite, T. D. (2022). Developmental coupling of cerebral blood flow and fMRI fluctuations in youth. *Cell Reports*, 38(13), 110576. <https://doi.org/10.1016/j.celrep.2022.110576>
- Beer, J. S., & Ochsner, K. N. (2006). Social cognition: A multi level analysis. *Brain Research*, 1079(1), 98–105. <https://doi.org/10.1016/j.brainres.2006.01.002>
- Bellucci, G., Chernyak, S. V., Goodyear, K., Eickhoff, S. B., & Krueger, F. (2017). Neural signatures of trust in reciprocity: A coordinate-based meta-analysis. *Human Brain Mapping*, 38(3), 1233–1248. <https://doi.org/10.1002/hbm.23451>
- Bellucci, G., Hahn, T., Deshpande, G., & Krueger, F. (2019). Functional connectivity of specific resting-state networks predicts trust and reciprocity in the trust game. *Cognitive, Affective, & Behavioral Neuroscience*, 19(1), 165–176. <https://doi.org/10.3758/s13415-018-00654-3>
- Berg, J., Dickhaut, J., & McCabe, K. (1995). Trust, reciprocity, and social history. *Games and Economic Behavior*, 10(1), 122–142. <http://doi.org/10.1006/game.1995.1027>
- Biotteau, M., Danna, J., Baudou, É., Puyjarinet, F., Velay, J. L., Albaret, J. M., & Chaix, Y. (2019). Developmental coordination disorder and dysgraphia: Signs and symptoms, diagnosis, and rehabilitation. *Neuropsychiatric Disease and Treatment*, 15, 1873–1885. <https://doi.org/10.2147/ndt.S120514>
- Birn, R. M., Molloy, E. K., Patriat, R., Parker, T., Meier, T. B., Kirk, G. R., Nair, V. A., Meyerand, M. E., & Prabhakaran, V. (2013). The effect of scan length on the reliability of resting-state fMRI connectivity estimates. *NeuroImage*, 83, 550–558. <https://doi.org/10.1016/j.neuroimage.2013.05.099>
- Biseco, A., Altieri, M., Santangelo, G., Di Nardo, F., Docimo, R., Caiazzo, G., Capuano, R., Pappacena, S., d'Ambrosio, A., Bonavita, S., Trojsi, F., Cirillo, M., Esposito, F., Tedeschi, G., & Gallo, A. (2019). Resting-state functional correlates of social cognition in multiple sclerosis: An explorative study. *Frontiers in Behavioral Neuroscience*, 13, 276. <https://doi.org/10.3389/fnbeh.2019.00276>
- Boksem, M. A., Mehta, P. H., Van den Bergh, B., van Son, V., Trautmann, S. T., Roelofs, K., Smidts, A., & Sanfey, A. G. (2013). Testosterone inhibits trust but promotes reciprocity. *Psychological Science*, 24(11), 2306–2314. <https://doi.org/10.1177/0956797613495063>
- Bowles, S., & Gintis, H. (2013). A cooperative species: Human reciprocity and its evolution. *Economics Books*, 50(3), 797–803. <https://doi.org/10.1515/9781400838837>
- Brandts, J., & Charness, G. (2011). The strategy versus the direct-response method: A first survey of experimental comparisons. *Experimental Economics*, 14(3), 375–398. <https://doi.org/10.1007/s10683-011-9272-x>
- Bressler, S. L., & Menon, V. (2010). Large-scale brain networks in cognition: Emerging methods and principles. *Trends in Cognitive Sciences*, 14(6), 277–290. <https://doi.org/10.1016/j.tics.2010.04.004>
- Brühlhart, M., & Usunier, J. C. (2012). Does the trust game measure trust? *Economics Letters*, 115(1), 20–23. <https://doi.org/10.1016/j.econlet.2011.11.039>
- Camerer C. (2003). *Behavioral game theory: Experiments in strategic interaction*. Princeton: Princeton University Press.
- Camerer, C., & Weigelt, K. (1988). Experimental tests of a sequential equilibrium reputation model. *Econometrica: Journal of the Econometric Society*, 56, 1–36. <http://www.jstor.org/stable/1911840>
- Cerullo, S., Fulceri, F., Muratori, F., & Contaldo, A. (2021). Acting with shared intentions: A systematic review on joint action coordination in autism spectrum disorder. *Brain and Cognition*, 149, 105693. <https://doi.org/10.1016/j.bandc.2021.105693>
- Chang, L. J., Gianaros, P. J., Manuck, S. B., Krishnan, A., & Wager, T. D. (2015). A sensitive and specific neural signature for picture-induced negative affect. *PLoS Biology*, 13(6), e1002180. <https://doi.org/10.1371/journal.pbio.1002180>
- Chang, L. J., Smith, A., Dufwenberg, M., & Sanfey, A. G. (2011). Triangulating the neural, psychological, and economic bases of guilt aversion. *Neuron*, 70(3), 560–572. <https://doi.org/10.1016/j.neuron.2011.02.056>
- Chen, X., Lu, B., & Yan, C. G. (2018). Reproducibility of R-fMRI metrics on the impact of different strategies for multiple comparison correction and sample sizes. *Human Brain Mapping*, 39(1), 300–318. <https://doi.org/10.1002/hbm.23843>
- Chen, X., Xu, Y., Li, B., Wu, X., Li, T., Wang, L., Zhang, Y., Lin, W., Quab, C., & Feng, C. (2021). Intranasal vasopressin modulates resting state brain activity across multiple neural systems: Evidence from a brain imaging machine learning study. *Neuropharmacology*, 190, 108561. <https://doi.org/10.1016/j.neuropharm.2021.108561>
- Cox, U., Di Martino, A., Castellanos, F. X., Milham, M. P., & Kelly, C. (2012). The balance between feeling and knowing: Affective and cognitive empathy are reflected in the brain's intrinsic functional dynamics. *Social Cognitive and Affective Neuroscience*, 7(6), 727–737. <https://doi.org/10.1093/scan/nsr051>
- Cox, J. C. (2004). How to identify trust and reciprocity. *Games and Economic Behavior*, 46(2), 260–281. [https://doi.org/10.1016/S0899-8256\(03\)00119-2](https://doi.org/10.1016/S0899-8256(03)00119-2)
- Cui, Z., & Gong, G. (2018). The effect of machine learning regression algorithms and sample size on individualized behavioral prediction with functional connectivity features. *NeuroImage*, 178, 622–637. <https://doi.org/10.1016/j.neuroimage.2018.06.001>
- Davis, J. D., Winkelman, P., & Coulson, S. (2017). Sensorimotor simulation and emotion processing: Impairing facial action increases semantic retrieval demands. *Cognitive, Affective, & Behavioral Neuroscience*, 17(3), 652–664. <https://doi.org/10.3758/s13415-017-0503-2>
- de la Vega, A., Yarkoni, T., Wager, T. D., & Banich, M. T. (2018). Large-scale Meta-analysis Suggests Low Regional Modularity in Lateral Frontal Cortex. *Cereb Cortex*, 28(10), 3414–3428. <https://doi.org/10.1093/cercor/bhx204>
- Declerck, C. H., Boone, C., & Emonds, G. (2013). When do people cooperate? The neuroeconomics of prosocial decision making. *Brain and Cognition*, 81(1), 95–117. <https://doi.org/10.1016/j.bandc.2012.09.009>

- Dubois, J., & Adolphs, R. (2016). Building a science of individual differences from fMRI. *Trends in Cognitive Sciences*, 20(6), 425–443. <https://doi.org/10.1016/j.tics.2016.03.014>
- Elliott, M. L., Knodt, A. R., & Hariri, A. R. (2021). Striving toward translation: Strategies for reliable fMRI measurement. *Trends in Cognitive Sciences*, 25(9), 776–787. <https://doi.org/10.1016/j.tics.2021.05.008>
- Falk, A., & Fischbacher, U. (2006). A theory of reciprocity. *Games and Economic Behavior*, 54(2), 293–315. <https://doi.org/10.2139/ssrn.203115>
- FeldmanHall, O., Son, J. Y., & Heffner, J. (2018). Norms and the flexibility of moral action. *Personal Neuroscience*, 1, e15. <https://doi.org/10.1017/pen.2018.13>
- Feng, C., Eickhoff, S. B., Li, T., Wang, L., Becker, B., Camilleri, J. A., Héту, S., & Luo, Y. (2021a). Common brain networks underlying human social interactions: Evidence from large-scale neuroimaging meta-analysis. *Neuroscience and Biobehavioral Reviews*, 126, 289–303. <https://doi.org/10.1016/j.neubiorev.2021.03.025>
- Feng, C., Zhu, Z., Cui, Z., Ushakov, V., Dreher, J. C., Luo, W., Gu, R., Wu, X., & Krueger, F. (2021b). Prediction of trust propensity from intrinsic brain morphology and functional connectome. *Human Brain Mapping*, 42(1), 175–191. <https://doi.org/10.1002/hbm.25215>
- Fett, A. K., Gromann, P. M., Giampietro, V., Shergill, S. S., & Krabbendam, L. (2014). Default distrust? An fMRI investigation of the neural development of trust and cooperation. *Social Cognitive and Affective Neuroscience*, 9(4), 395–402. <https://doi.org/10.1093/scan/nss144>
- Finn, E. S., Shen, X., Scheinost, D., Rosenberg, M. D., Huang, J., Chun, M. M., Papademetris, X., & Constable, R. T. (2015). Functional connectome fingerprinting: Identifying individuals using patterns of brain connectivity. *Nature Neuroscience*, 18(11), 1664–1671. <https://doi.org/10.1038/nn.4135>
- Friston, K. J., Williams, S., Howard, R., Frackowiak, R. S., & Turner, R. (1996). Movement-related effects in fMRI time-series. *Magnetic Resonance in Medicine*, 35(3), 346–355. <https://doi.org/10.1002/mrm.1910350312>
- Gong, X., Brazil, I. A., Chang, L. J., & Sanfey, A. G. (2019). Psychopathic traits are related to diminished guilt aversion and reduced trustworthiness during social decision-making. *Scientific Reports*, 9(1), 7307. <https://doi.org/10.1038/s41598-019-43727-0>
- Hahn, T., Notebaert, K., Anderl, C., Reicherts, P., Wieser, M., Kopf, J., Reif, A., Fehl, K., Semmann, D., & Windmann, S. (2015). Reliance on functional resting-state network for stable task control predicts behavioral tendency for cooperation. *NeuroImage*, 118, 231–236. <https://doi.org/10.1016/j.neuroimage.2015.05.093>
- Haufe, S., Meinecke, F., Görgen, K., Dähne, S., Haynes, J. D., Blankertz, B., & Bießmann, F. (2014). On the interpretation of weight vectors of linear models in multivariate neuroimaging. *NeuroImage*, 87, 96–110. <https://doi.org/10.1016/j.neuroimage.2013.10.067>
- He, Y., & Evans, A. (2010). Graph theoretical modeling of brain connectivity. *Current Opinion in Neurology*, 23(4), 341–350. <https://doi.org/10.1097/WCO.0b013e32833aa567>
- He, Y., Wang, J., Wang, L., Chen, Z. J., Yan, C., Yang, H., Tang, H., Zhu, C., Gong, Q., Zang, Y., & Evans, A. C. (2009). Uncovering intrinsic modular organization of spontaneous brain activity in humans. *PLoS One*, 4(4), e5226. <https://doi.org/10.1371/journal.pone.0005226>
- Heffner, J., Vives, M. L., & FeldmanHall, O. (2021). Emotional responses to prosocial messages increase willingness to self-isolate during the COVID-19 pandemic. *Personality and Individual Differences*, 170, 110420. <https://doi.org/10.1016/j.paid.2020.110420>
- Hoerl, A. E., & Kennard, R. W. (1970). Ridge regression: Biased estimation for nonorthogonal problems. *Technometrics*, 12(1), 55–67. <https://doi.org/10.1080/00401706.1970.10488634>
- Holiga, Š., Sambataro, F., Luzy, C., Greig, G., Sarkar, N., Renken, R. J., Marsman, J.-B. C., Schobel, S. A., Bertolino, A., & Dukart, J. (2018). Test-retest reliability of task-based and resting-state blood oxygen level dependence and cerebral blood flow measures. *PLoS One*, 13(11), e0206583. <https://doi.org/10.1371/journal.pone.0206583>
- Hoptman, M. J., Zuo, X. N., Butler, P. D., Javitt, D. C., D'Angelo, D., Mauro, C. J., & Milham, M. P. (2010). Amplitude of low-frequency oscillations in schizophrenia: A resting state fMRI study. *Schizophrenia Research*, 117(1), 13–20. <https://doi.org/10.1016/j.schres.2009.09.030>
- Hsu, W. T., Rosenberg, M. D., Scheinost, D., Constable, R. T., & Chun, M. M. (2018). Resting-state functional connectivity predicts neuroticism and extraversion in novel individuals. *Social Cognitive and Affective Neuroscience*, 13(2), 224–232. <https://doi.org/10.1093/scan/nsy002>
- Iacoboni, M., & Dapretto, M. (2006). The mirror neuron system and the consequences of its dysfunction. *Nature Reviews. Neuroscience*, 7(12), 942–951. <https://doi.org/10.1038/nrn2024>
- Ibáñez, M. I., Sabater-Grande, G., Barreda-Tarrazona, I., Mezquita, L., López-Ovejero, S., Villa, H., Perakakis, P., Ortet, G., García-Gallego, A., & Georgantzis, N. (2016). Take the money and run: Psychopathic behavior in the trust game. *Frontiers in Psychology*, 7, 1866. <https://doi.org/10.3389/fpsyg.2016.01866>
- Ikeda, S., Takeuchi, H., Taki, Y., Nouchi, R., Yokoyama, R., Kotozaki, Y., Nakagawa, S., Sekiguchi, A., Iizuka, K., Yamamoto, Y., Hanawa, S., Araki, T., Miyachi, C. M., Sakaki, K., Nozawa, T., Yokota, S., Magistro, D., & Kawashima, R. (2017). A comprehensive analysis of the correlations between resting-state oscillations in multiple-frequency bands and big five traits. *Frontiers in Human Neuroscience*, 11, 321. <https://doi.org/10.3389/fnhum.2017.00321>
- Kable, J. W., & Levy, I. (2015). Neural markers of individual differences in decision-making. *Current Opinion in Behavioral Sciences*, 5, 100–107. <https://doi.org/10.1016/j.cobeha.2015.08.004>
- Kanai, R., & Rees, G. (2011). The structural basis of inter-individual differences in human behaviour and cognition. *Nature Reviews. Neuroscience*, 12(4), 231–242. <https://doi.org/10.1038/nrn3000>
- Karlaftis, V. M., Giorgio, J., Vértes, P. E., Wang, R., Shen, Y., Tino, P., Welchman, A. E., & Kourtzi, Z. (2019). Multimodal imaging of brain connectivity reveals predictors of individual decision strategy in statistical learning. *Nature Human Behaviour*, 3, 297–307. <https://doi.org/10.1038/s41562-018-0503-4>
- Kilroy, E., Cermak, S. A., & Aziz-Zadeh, L. (2019). A review of functional and structural neurobiology of the action observation network in autism spectrum disorder and developmental coordination disorder. *Brain Sciences*, 9(4), 75. <https://doi.org/10.3390/brainsci9040075>
- King-Casas, B., Tomlin, D., Anen, C., Camerer, C. F., Quartz, S. R., & Montague, P. R. (2005). Getting to know you: Reputation and trust in a two-person economic exchange. *Science*, 308(5718), 78–83. <https://doi.org/10.1126/science.1108062>
- Knoch, D., Schneider, F., Schunk, D., Hohmann, M., & Fehr, E. (2009). Disrupting the prefrontal cortex diminishes the human ability to build a good reputation. *Proceedings of the National Academy of Sciences of the United States of America*, 106(49), 20895–20899. <https://doi.org/10.1073/pnas.0911619106>
- Kohoutová, L., Heo, J., Cha, S., Lee, S., Moon, T., Wager, T. D., & Woo, C. W. (2020). Toward a unified framework for interpreting machine-learning models in neuroimaging. *Nature Protocols*, 15(4), 1399–1435. <https://doi.org/10.1038/s41596-019-0289-5>
- Krueger, F., Bellucci, G., Xu, P., & Feng, C. (2020). The critical role of the right dorsal and ventral anterior insula in reciprocity: Evidence from the trust and ultimatum games. *Frontiers in Human Neuroscience*, 14, 176. <https://doi.org/10.3389/fnhum.2020.00176>
- Krueger, F., Grafman, J., & McCabe, K. (2008). Neural correlates of economic game playing. *Philosophical Transactions of the Royal Society of London. Series B, Biological Sciences*, 363(1511), 3859–3874. <https://doi.org/10.1098/rstb.2008.0165>
- Krueger, F., McCabe, K., Moll, J., Kriegeskorte, N., Zahn, R., Strenziok, M., Heinecke, A., & Grafman, J. (2007). Neural correlates of trust.

- Proceedings of the National Academy of Sciences of the United States of America*, 104(50), 20084–20089. <https://doi.org/10.1073/pnas.0710103104>
- Kunisato, Y., Okamoto, Y., Okada, G., Aoyama, S., Nishiyama, Y., Onoda, K., & Yamawaki, S. (2011). Personality traits and the amplitude of spontaneous low-frequency oscillations during resting state. *Neuroscience Letters*, 492(2), 109–113. <https://doi.org/10.1016/j.neulet.2011.01.067>
- Li, T., Yang, Y., Krueger, F., Feng, C., & Wang, J. (2021). Static and dynamic topological organizations of the costly punishment network predict individual differences in punishment propensity. *Cerebral Cortex*. Online ahead of print. <https://doi.org/10.1093/cercor/bhab462>
- Li, Z., Zhu, Y., Childress, A. R., Detre, J. A., & Wang, Z. (2012). Relations between BOLD fMRI-derived resting brain activity and cerebral blood flow. *PLoS One*, 7(9), e44556. <https://doi.org/10.1371/journal.pone.0044556>
- Lu, X., Li, T., Xia, Z., Zhu, R., Wang, L., Luo, Y. J., Feng, C., & Krueger, F. (2019). Connectome-based model predicts individual differences in propensity to trust. *Human Brain Mapping*, 40(6), 1942–1954. <https://doi.org/10.1002/hbm.24503>
- Mccabe, K. A., Rigdon, M. L., & Smith, V. L. (2003). Positive reciprocity and intentions in trust games. *Journal of Economic Behavior & Organization*, 52(2), 267–275. [https://doi.org/10.1016/S0167-2681\(03\)00003-9](https://doi.org/10.1016/S0167-2681(03)00003-9)
- Mišić, B., & Sporns, O. (2016). From regions to connections and networks: New bridges between brain and behavior. *Current Opinion in Neurobiology*, 40, 1–7. <https://doi.org/10.1016/j.conb.2016.05.003>
- Nash, K., & Knoch, D. (2016). *Individual differences in decision-making: A neural trait approach to study sources of behavioral heterogeneity*. Springer Berlin Heidelberg.
- Nash, K., Gianotti, L. R., & Knoch, D. (2014). A neural trait approach to exploring individual differences in social preferences. *Frontiers in Behavioral Neuroscience*, 8, 458. <https://doi.org/10.3389/fnbeh.2014.00458>
- Nihonusugi, T., Ihara, A., & Haruno, M. (2015). Selective increase of intention-based economic decisions by noninvasive brain stimulation to the dorsolateral prefrontal cortex. *The Journal of Neuroscience*, 35(8), 3412–3419. <https://doi.org/10.1523/jneurosci.3885-14.2015>
- Nishina, K., Takagishi, H., Takahashi, H., Sakagami, M., & Inoue-Murayama, M. (2019). Association of polymorphism of arginine-vasopressin receptor 1A (AVPR1a) gene with trust and reciprocity. *Frontiers in Human Neuroscience*, 13, 230. <https://doi.org/10.3389/fnhum.2019.00230>
- Oldehinkel, M., Mennes, M., Marquand, A., Charman, T., Tillmann, J., Ecker, C., Dell'Acqua, F., Brandeis, D., Banaschewski, T., Baumeister, S., Moessnang, C., Baron-Cohen, S., Holt, R., Bölte, S., Durston, S., Kundu, P., Lombardo, M. V., Spooren, W., Loth, E., ... Buitelaar, J. K. (2019). Altered connectivity between cerebellum, visual, and sensory-motor networks in autism spectrum disorder: Results from the EU-AIMS longitudinal European Autism Project. *Biological Psychiatry: Cognitive Neuroscience and Neuroimaging*, 4(3), 260–270. <https://doi.org/10.1016/j.bpsc.2018.11.010>
- Oliver, L. D., Vieira, J. B., Neufeld, R. W. J., Dziobek, I., & Mitchell, D. G. V. (2018). Greater involvement of action simulation mechanisms in emotional vs cognitive empathy. *Social Cognitive and Affective Neuroscience*, 13(4), 367–380. <https://doi.org/10.1093/scan/nsy013>
- Peysakhovich, A., Nowak, M. A., & Rand, D. G. (2014). Humans display a “cooperative phenotype” that is domain general and temporally stable. *Nature Communications*, 5, 4939. <https://doi.org/10.1038/ncomms5939>
- Phelps, E. A., Lempert, K. M., & Sokol-Hessner, P. (2014). Emotion and decision making: Multiple modulatory neural circuits. *Annual Review of Neuroscience*, 37, 263–287. <https://doi.org/10.1146/annurev-neuro-071013-014119>
- Pineda, J. A. (2008). Sensorimotor cortex as a critical component of an “extended” mirror neuron system: Does it solve the development, correspondence, and control problems in mirroring? *Behavioral and Brain Functions*, 4, 47. <https://doi.org/10.1186/1744-9081-4-47>
- Power, J. D., Barnes, K. A., Snyder, A. Z., Schlaggar, B. L., & Petersen, S. E. (2012). Spurious but systematic correlations in functional connectivity MRI networks arise from subject motion. *NeuroImage*, 59(3), 2142–2154. <https://doi.org/10.1016/j.neuroimage.2011.10.018>
- Power, J. D., Cohen, A. L., Nelson, S. M., Wig, G. S., Barnes, K. A., Church, J. A., Vogel, A. C., Laumann, T. O., Miezin, F. M., Schlaggar, B. L., & Petersen, S. E. (2011). Functional network organization of the human brain. *Neuron*, 72(4), 665–678. <https://doi.org/10.1016/j.neuron.2011.09.006>
- Power, J. D., Schlaggar, B. L., Lessov-Schlaggar, C. N., & Petersen, S. E. (2013). Evidence for hubs in human functional brain networks. *Neuron*, 79(4), 798–813. <https://doi.org/10.1016/j.neuron.2013.07.035>
- Rand, D. G., & Nowak, M. A. (2013). Human cooperation. *Trends in Cognitive Sciences*, 17(8), 413–425. <https://doi.org/10.1016/j.tics.2013.06.003>
- Rilling, J. K., Goldsmith, D. R., Glenn, A. L., Jairam, M. R., Elfenbein, H. A., Dagenais, J. E., Murdock, C. D., & Pagnoni, G. (2008). The neural correlates of the affective response to unreciprocated cooperation. *Neuropsychologia*, 46(5), 1256–1266. <https://doi.org/10.1016/j.neuropsychologia.2007.11.033>
- Rilling, J. K., Sanfey, A. G., Aronson, J. A., Nystrom, L. E., & Cohen, J. D. (2004). Opposing BOLD responses to reciprocated and unreciprocated altruism in putative reward pathways. *Neuroreport*, 15(16), 2539–2543. <https://doi.org/10.1097/00001756-200411150-00022>
- Romano, A., Balliet, D., Yamagishi, T., & Liu, J. H. (2017). Parochial trust and cooperation across 17 societies. *Proceedings of the National Academy of Sciences of the United States of America*, 114(48), 12702–12707. <https://doi.org/10.1073/pnas.1712921114>
- Rosenberg, M. D., Finn, E. S., Scheinost, D., Papademetris, X., Shen, X., Constable, R. T., & Chun, M. M. (2016). A neuromarker of sustained attention from whole-brain functional connectivity. *Nature Neuroscience*, 19(1), 165–171. <https://doi.org/10.1038/nn.4179>
- Rubinov, M., & Sporns, O. (2010). Complex network measures of brain connectivity: Uses and interpretations. *NeuroImage*, 52(3), 1059–1069. <https://doi.org/10.1016/j.neuroimage.2009.10.003>
- Schilbach, L., Timmermans, B., Reddy, V., Costall, A., Bente, G., Schlicht, T., & Vogeley, K. (2013). Toward a second-person neuroscience. *The Behavioral and Brain Sciences*, 36(4), 393–414. <https://doi.org/10.1017/s0140525x12000660>
- Schreiner, M. J., Karlsgodt, K. H., Uddin, L. Q., Chow, C., Congdon, E., Jalbrzikowski, M., & Bearden, C. E. (2014). Default mode network connectivity and reciprocal social behavior in 22q11.2 deletion syndrome. *Social Cognitive and Affective Neuroscience*, 9(9), 1261–1267. <https://doi.org/10.1093/scan/nst114>
- Siegel, J. S., Ramsey, L. E., Snyder, A. Z., Metcalf, N. V., Chacko, R. V., Weinberger, K., Baldassarre, A., Hacker, C. D., Shulman, G. L., & Corbetta, M. (2016). Disruptions of network connectivity predict impairment in multiple behavioral domains after stroke. *Proceedings of the National Academy of Sciences*, 113(30), E4367–E4376. <https://doi.org/10.1073/pnas.1521083113>
- Somandepalli, K., Kelly, C., Reiss, P. T., Zuo, X. N., Craddock, R. C., Yan, C. G., Petkova, E., Castellanos, F. X., Milham, M. P., & Di Martino, A. (2015). Short-term test-retest reliability of resting state fMRI metrics in children with and without attention-deficit/hyperactivity disorder. *Developmental Cognitive Neuroscience*, 15, 83–93. <https://doi.org/10.1016/j.dcn.2015.08.003>
- Song, D., Chang, D., Zhang, J., Ge, Q., Zang, Y. F., & Wang, Z. (2019). Associations of brain entropy (BEN) to cerebral blood flow and fractional amplitude of low-frequency fluctuations in the resting brain. *Brain Imaging and Behavior*, 13(5), 1486–1495. <https://doi.org/10.1007/s11682-018-9963-4>

- Tangney, J. P., Stuewig, J., & Mashek, D. J. (2007). Moral emotions and moral behavior. *Annual Review of Psychology*, 58, 345–372. <https://doi.org/10.1146/annurev.psych.56.091103.070145>
- Tomasí, D., Wang, G. J., & Volkow, N. D. (2013). Energetic cost of brain functional connectivity. *Proceedings of the National Academy of Sciences of the United States of America*, 110(33), 13642–13647. <https://doi.org/10.1073/pnas.1303346110>
- van den Bos, W., van Dijk, E., Westenberg, M., Rombouts, S. A., & Crone, E. A. (2009). What motivates repayment? Neural correlates of reciprocity in the trust game. *Social Cognitive and Affective Neuroscience*, 4(3), 294–304. <https://doi.org/10.1093/scan/nsp009>
- van den Bos, W., van Dijk, E., Westenberg, M., Rombouts, S. A., & Crone, E. A. (2011). Changing brains, changing perspectives: The neurocognitive development of reciprocity. *Psychological Science*, 22(1), 60–70. <https://doi.org/10.1177/0956797610391102>
- Varoquaux, G., Raamana, P. R., Engemann, D. A., Hoyos-Ildrobo, A., Schwartz, Y., & Thirion, B. (2017). Assessing and tuning brain decoders: Cross-validation, caveats, and guidelines. *NeuroImage*, 145 (Pt B), 166–179. <https://doi.org/10.1016/j.neuroimage.2016.10.038>
- Vinod, H. D. (1978). A survey of ridge regression and related techniques for improvements over ordinary least squares. *The Review of Economics and Statistics*, 60(1), 121–131. <https://doi.org/10.2307/1924340>
- Wager, T. D., Atlas, L. Y., Lindquist, M. A., Roy, M., Woo, C. W., & Kross, E. (2013). An fMRI-based neurologic signature of physical pain. *The New England Journal of Medicine*, 368(15), 1388–1397. <https://doi.org/10.1056/NEJMoa1204471>
- Wagner, U., N'Diaye, K., Ethofer, T., & Vuilleumier, P. (2011). Guilt-specific processing in the prefrontal cortex. *Cerebral Cortex*, 21(11), 2461–2470. <https://doi.org/10.1093/cercor/bhr016>
- Wang, J., Wang, X., Xia, M., Liao, X., Evans, A., & He, Y. (2015). GREYNA: A graph theoretical network analysis toolbox for imaging connectomics. *Frontiers in Human Neuroscience*, 9(386), 386. <https://doi.org/10.3389/fnhum.2015.00386>
- Woo, C. W., Koban, L., Kross, E., Lindquist, M. A., Banich, M. T., Ruzic, L., Andrews-Hanna, J. R., & Wager, T. D. (2014). Separate neural representations for physical pain and social rejection. *Nature Communications*, 5, 5380. <https://doi.org/10.1038/ncomms6380>
- Woo, C. W., Schmidt, L., Krishnan, A., Jepma, M., Roy, M., Lindquist, M. A., Atlas, L. Y., & Wager, T. D. (2017). Quantifying cerebral contributions to pain beyond nociception. *Nature Communications*, 8, 14211. <https://doi.org/10.1038/ncomms14211>
- Xu, Y., Lin, Q., Han, Z., He, Y., & Bi, Y. (2016). Intrinsic functional network architecture of human semantic processing: Modules and hubs. *NeuroImage*, 132, 542–555. <https://doi.org/10.1016/j.neuroimage.2016.03.004>
- Yan, C.-G. (2010). DPARSF: A MATLAB toolbox for “pipeline” data analysis of resting-state fMRI. *Frontiers in Systems Neuroscience*, 4, 13. <https://doi.org/10.3389/fnsys.2010.00013>
- Yan, C. G., Cheung, B., Kelly, C., Colcombe, S., Craddock, R. C., Martino, A. D., Li, Q., Zuo, X.-N., Castellanos, F. X., & Milham, M. P. (2013). A comprehensive assessment of regional variation in the impact of head micromovements on functional connectomics. *NeuroImage*, 76(1), 183–201. <https://doi.org/10.1016/j.neuroimage.2013.03.004>
- Yan, C.-G., Wang, X.-D., Zuo, X.-N., & Zang, Y.-F. (2016). DPABI: Data processing & analysis for (resting-state) brain imaging. *Neuroinformatics*, 14(3), 339–351. <https://doi.org/10.1007/s12021-016-9299-4>
- Yang, D., Pelphrey, K. A., Sukhodolsky, D. G., Crowley, M. J., Dayan, E., Dvornek, N. C., Venkataraman, A., Duncan, J., Staib, L., & Ventola, P. (2016). Brain responses to biological motion predict treatment outcome in young children with autism. *Translational Psychiatry*, 6(11), e948. <https://doi.org/10.1038/tp.2016.213>
- Yarkoni, T., Poldrack, R. A., Nichols, T. E., Van Essen, D. C., & Wager, T. D. (2011). Large-scale automated synthesis of human functional neuroimaging data. *Nature Methods*, 8(8), 665–670. <https://doi.org/10.1038/nmeth.1635>
- Yu-Feng, Z., Yong, H., Chao-Zhe, Z., Qing-Jiu, C., Man-Qiu, S., Meng, L., Tian, L.-X., Jiang, T.-Z., & Yu-Feng, W. (2007). Altered baseline brain activity in children with ADHD revealed by resting-state functional MRI. *Brain and Development*, 29(2), 83–91. <https://doi.org/10.1016/j.braindev.2006.07.002>
- Zhao, K., & Smillie, L. D. (2015). The role of interpersonal traits in social decision making: Exploring sources of behavioral heterogeneity in economic games. *Personality and Social Psychology Review*, 19(3), 277–302. <https://doi.org/10.1177/1088868314553709>
- Zou, Q.-H., Zhu, C. Z., Yang, Y., Zuo, X. N., Long, X. Y., Cao, Q. J., Wang, Y.-F., & Zang, Y. F. (2008). An improved approach to detection of amplitude of low-frequency fluctuation (ALFF) for resting-state fMRI: Fractional ALFF. *Journal of Neuroscience Methods*, 172(1), 137–141. <https://doi.org/10.1016/j.jneumeth.2008.04.012>
- Zuo, X. N., Di Martino, A., Kelly, C., Shehzad, Z. E., Gee, D. G., Klein, D. F., Castellanos, F. X., Biswal, B. B., & Milham, M. P. (2010). The oscillating brain: Complex and reliable. *NeuroImage*, 49(2), 1432–1445. <https://doi.org/10.1016/j.neuroimage.2009.09.037>
- Zuo, X. N., & Xing, X. X. (2014). Test-retest reliabilities of resting-state fMRI measurements in human brain functional connectomics: A systems neuroscience perspective. *Neuroscience and Biobehavioral Reviews*, 45, 100–118. <https://doi.org/10.1016/j.neubiorev.2014.05.009>

How to cite this article: Li, T., Pei, Z., Zhu, Z., Wu, X., & Feng, C. (2022). Intrinsic brain activity patterns across large-scale networks predict reciprocity propensity. *Human Brain Mapping*, 43(18), 5616–5629. <https://doi.org/10.1002/hbm.26038>